



Received on 15 April 2019; received in revised form, 07 August 2019; accepted, 13 August 2019; published 01 January 2020

## ADSORPTION OF CIPROFLOXACIN FROM AQUEOUS SOLUTION ONTO $Fe_3O_4$ /GRAPHENE OXIDE NANOCOMPOSITE

Davoud Balarak<sup>1</sup>, Mohadeseh Zafariyan<sup>2</sup> and Kethineni Chandrika<sup>\*3</sup>

Department of Environmental Health, Health Promotion Research Center<sup>1</sup>, Student Research Committee<sup>2</sup>, Zahedan University of Medical Sciences, Zahedan, Iran.

Department of Biotechnology<sup>3</sup>, Koneru Lakshmaiah Education Foundation, Vaddeswaram, Guntur - 522502, Andhra Pradesh, India.

### Keywords:

$Fe_3O_4$ -graphene oxide,  
Ciprofloxacin, Kinetics,  
Thermodynamic

### Correspondence to Author:

**Kethineni Chandrika**

Associate Professor,  
Department of Biotechnology,  
Koneru Lakshmaiah Education  
Foundation, Vaddeswaram, Guntur -  
522502, Andhra Pradesh, India.

**E-mail:** [kkchandrika@kluniversity.in](mailto:kkchandrika@kluniversity.in)

**ABSTRACT:** In this research, ciprofloxacin adsorption (CIP) onto graphene oxide synthesized with  $Fe_3O_4$  ( $Fe_3O_4$ -GO) was applied *via* various adsorbent dose, contact time, temperature and initial CIP concentration. The results showed that the percentage removal of CIP decreases from 98.1 to %77.4, as the CIP concentration increases from 25 to 200 mg/L. Also, the amount of CIP adsorbed per unit mass of adsorbent increased from 49.25 to 309.6 mg/g with increasing in CIP concentration from 25 to 200 mg/L. The results showed that the adsorption was accurately represented by the pseudo-second-order model. Under different temperature, the CIP maximum adsorption on  $Fe_3O_4$ -GO calculated by pseudo-second-order kinetic model and were 197 mg/g (273 K), 191.6 mg/g (288 K), 182.2 mg/g (303 K) and 172.6 mg/g (318 K). Also, the results showed the existence of three steps during the adsorption process. The first stage was the transport of CIP molecule from the adsorbents external surface to the pores of the adsorbent internal structure. The second stage is the transport of CIP molecule from the adsorbent external surface to the pores of the adsorbent internal structure. The third stage is the adsorption of CIP molecule on the interior surface of the adsorbent. The results suggest that  $Fe_3O_4$ -GO could be employed as an effective material for the removal of CIP from aqueous solutions.

**INTRODUCTION:** Contamination of surface and even groundwater is becoming an increasingly serious problem worldwide because of the growing population and widespread use of chemicals, including pharmaceuticals<sup>1-3</sup>. The pharmaceuticals constitute an important and rapidly emerging class of pollutants worldwide<sup>4,5</sup>.

Pharmaceutical compounds have been recognized as a hazardous class of organic pollutants due to their extensive use and long term effects towards aquatic environment<sup>6,7</sup>. Antibiotics constitute a group of pharmaceuticals that are widely used to treat several infectious diseases in both human and animals<sup>8</sup>. About 30-90% of the given antibiotic dose can remain undegradable in the human or animal body and is largely excreted as an active compound<sup>9,10</sup>.

Most antibiotics are incompletely metabolized; thus, their residues and degradation products are excreted and can enter water environments in various ways<sup>11,12</sup>. Exposure to the residues and

	<b>QUICK RESPONSE CODE</b> <b>DOI:</b> 10.13040/IJPSR.0975-8232.11(1).268-74
	The article can be accessed online on <a href="http://www.ijpsr.com">www.ijpsr.com</a>
<b>DOI link:</b> <a href="http://dx.doi.org/10.13040/IJPSR.0975-8232.11(1).268-74">http://dx.doi.org/10.13040/IJPSR.0975-8232.11(1).268-74</a>	

metabolites of antibiotics may cause a variety of adverse effects in the environment, such as antibiotics resistance of microorganisms and chronic and acute toxicity for organisms<sup>13, 14</sup>. Among the antibiotics used, Ciprofloxacin (CIP) antibiotics are belonging to the Fluoroquinolones (FQs) family, are hydrolytically stable, difficult to degrade in water and widely detected in wastewater, soil and sediments<sup>15, 16</sup>. Environmental risks associated with SIP including antibiotic resistance of bacteria have been reported<sup>17</sup>. Pharmaceuticals are emerging contaminants and their effective removal from water resources is very important<sup>18</sup>. The efficiency of antibiotics removal from water in a traditional system is low because of their low biodegradability, high solubility in water, and complex molecular structures<sup>19, 20, 21</sup>.

Therefore, various methods such as ozonation, oxidation, reduction, gamma-ray irradiation, photolysis, and adsorption have been suggested as potential and competitive methods to remove antibiotics from water<sup>22, 23, 24</sup>. Of these processes, it has been demonstrated that adsorption is a simple, effective, and economical method to remove pollutants from waters<sup>25, 26</sup>. Adsorption is the widely used method for removal of a broad range of antibiotics pollutants due to its simple design, easy operation, and relatively simple regeneration<sup>27</sup>. Currently, nanomaterials have been used by researchers to advance the removal and treatment of industrial wastewaters<sup>28</sup>.

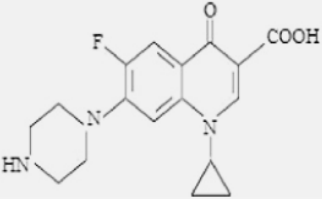
These nanomaterials are divided into two main categories such as nanometal and none-nano metal materials such as Fe<sub>3</sub>O<sub>4</sub>-graphene oxide (Fe<sub>3</sub>O<sub>4</sub>-GO) and graphene oxide or nano-carbon families, which are powerful and remarkable nanomaterials that could be used as a strong absorbent via their great and enormous specific surface area and minor internal diffusion resistance<sup>29</sup>.

In present work, Fe<sub>3</sub>O<sub>4</sub>-GO was prepared to create a strong adsorbent with low prices and simple synthesis procedure to adsorb and separate the ciprofloxacin antibiotics from aqueous solution. The adsorption manner of CIP onto Fe<sub>3</sub>O<sub>4</sub>-GO nanocomposite was explored and the main adsorption mechanisms were surveyed in different initial CIP concentration, contact time, adsorbent dose and temperatures.

## MATERIALS AND METHODS:

**Materials:** All chemical materials used were of analytical reagent grade and used without further purification. Analytical grade CIP was obtained from Sigma Aldrich Co., and used as received; its characteristics are given in **Table 1**. Graphene oxide nanoparticles were manufactured by improved Hummers method<sup>29</sup>.

**TABLE 1: CHARACTERISTICS AND STRUCTURE OF CIPROFLOXACIN**

Weight	331.35 g/mol
Formula	C <sub>17</sub> H <sub>18</sub> FN <sub>3</sub> O <sub>3</sub>
Structure	
Solubility at water	150–6190 mg/L
$\lambda_{\max}$	270 nm

**Preparation of Graphene Oxide:** Graphene oxide was prepared from graphite powder using a modified Hummer's method. Firstly, a 9:1 mixture of concentrated H<sub>2</sub>SO<sub>4</sub>: H<sub>3</sub>PO<sub>4</sub> was added to a mixture of graphite flake (3 g, 1 wt equivalent) and KMnO<sub>4</sub> (18 g, 6 wt), producing a slight exothermal to 35-40 °C. Then the reaction was washed and the residues were centrifuged (4000 rpm for 4 h) and the supernatant decanted away. The remaining material after the multiple-wash process was mixed with 200 mL of diethyl ether. The obtained solid on the filter was vacuum-dried overnight at room temperature.

**Preparation of Fe<sub>3</sub>O<sub>4</sub>-GO Nanocomposite:** Firstly 15 mL of graphene oxide (2.72 mg/mL) was dispersed into 40 mL ethanol with stirring. Then 0.9522 g of FeCl<sub>3</sub>•6H<sub>2</sub>O (3.5228 mmol) and 1.0520 g of FeSO<sub>4</sub>•7H<sub>2</sub>O (3.7842 mmol) were dissolved in 10 mL of distilled water under sonication and solution was injected dropwise into the graphene oxide suspension and stirred for 0.5 h. The resulting mixture was heated to 68 °C before the ammonia solution was added to adjust the pH to 10. The mixture was stirred at 68 °C for 2 h and cooled to room temperature. The Fe<sub>3</sub>O<sub>4</sub>-GO composite was separated from the mixture using a permanent magnet and rinsed two times with ethanol and distilled water, respectively before being dried at 65 °C for 12 h.

**Adsorption Study:** Batch adsorption experiments were carried out using a shaker. The effects of contact time, CIP concentration, adsorbent dose and temperature on adsorption were investigated. For each experimental run, 0.5 g adsorbent and 100 mL of CIP solution of known concentration were transferred into a flask and agitated by shaker at a constant speed of 180 rpm with a required adsorption time. At predetermined time intervals, the solutions were centrifuged at 3600 rpm for 10 min. The adsorption kinetics was determined by analyzing adsorption capacity from the aqueous solution at different time intervals. Kinetics solution of different concentrations in the range of 273-318 K was agitated until the equilibrium was achieved.

Concentrations of CIP were determined by finding out the absorbance characteristic wavelength using UV-spectrophotometer. A standard solution of the CIP was taken and the absorbance was determined at different wavelengths to obtain a plot of absorbance versus wavelength. The wavelength corresponding to maximum absorbance ( $\lambda_{\max}$ ) was determined from this plot. The  $\lambda_{\max}$  for CIP was found to be 270 nm. Calibration curves were

plotted between absorbance and concentration of the CIP solution. The adsorbed amount ( $q_e$ ) of CIP was calculated by the following equation:<sup>30</sup>

$$q_e = ((C_0 - C_e) \times V) / M$$

Where,  $C_0$  and  $C_e$  are the initial and equilibrium concentrations of CIP (mg/L),  $m$  is the mass of sorbent (g), and  $V$  is the volume of solution (L).

## RESULTS AND DISCUSSION:

**Effect of Initial CIP Concentration and Contact Time:** The initial concentration of CIP in solution provides an important driving force in overcoming mass transfer resistance between the aqueous and the solid phases<sup>24</sup>. Equilibrium adsorption studies have been performed to determine the capacity of the adsorbent, and the equilibrium is established when the concentration of adsorbate in the bulk solution is in dynamic balance with that on the surface<sup>30</sup>. The effect of initial CIP concentration is shown in **Fig. 1**. For 0.6 g/L of adsorbent, the percentage removal of CIP decreases from 98.1 to 77.4% as the CIP concentration increases from 25 to 200 mg/L. But, the amount of CIP adsorbed per unit mass of adsorbent increased with increasing in CIP concentration **Fig 2**.

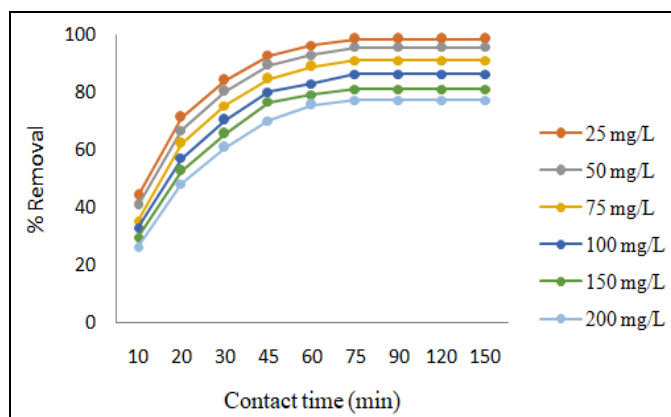


**FIG. 1: EFFECT OF INITIAL CIP CONCENTRATION AND CONTACT TIME**  
(Dose= 0.6 g/L, pH = 7, and Temp= 25 °C)

This may be due to all CIP there in solution could intermingle with the binding sites at lower concentration and thus the percentage adsorption was higher than those at higher initial CIP concentration<sup>31, 32</sup>. At higher concentrations, lower adsorption yield is due to the saturation of adsorption sites<sup>33</sup>. At low concentrations, sorption sites took up the available CIP molecule more rapidly while at higher concentrations the rate of diffusion became slow<sup>33, 34</sup>. The effect of contact

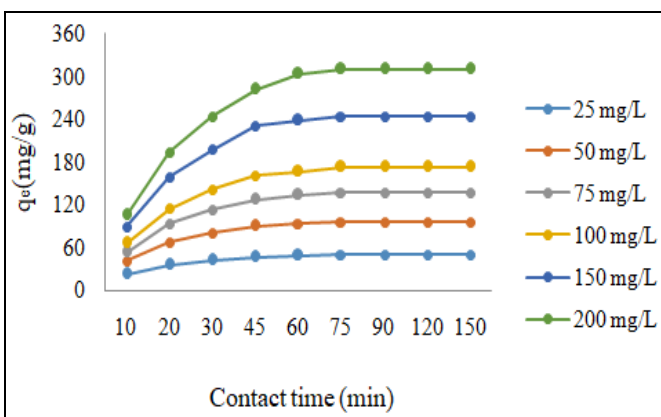


**FIG. 2: EFFECT OF INITIAL CIP CONCENTRATION AND CONTACT TIME ON ADSORPTION CAPACITY**  
(Dose= 0.6 g/L, pH = 7, and Temp= 25 °C)

time on the removal of CIP onto Fe<sub>3</sub>O<sub>4</sub>-GO for different concentration of CIP is shown in **Fig. 2**. The results revealed that the rate of CIP removal is higher at the beginning, which was due to the large available surface area<sup>35</sup>.

As the surface adsorption sites become exhausted, the uptake rate is controlled by the rate at which the adsorbate is transported from the exterior to interior sites of the adsorbent. Almost 70% of the total CIP

molecule was adsorbed in the initial 10 min period and remained almost unchanged after 75 min, indicating that the adsorption process has reached equilibrium.

**Effect of Adsorbent Dosage:** The effect of changing the adsorbent dosage on the removal of CIP was studied by varying the adsorbent dosage from 0.1 to 0.9 g/L while keeping the other experimental conditions as constant **Fig. 3**.

An increase in percentage removal of CIP with increasing adsorbent dosage was observed whereas the adsorption capacity for the adsorbents decreased. This is due to the larger surface area and availability of more surface functional groups at higher concentration of adsorbent<sup>36, 37</sup>. The decrease in adsorption capacity can be explained with the reduction in effective surface area of the adsorbent<sup>38</sup>.

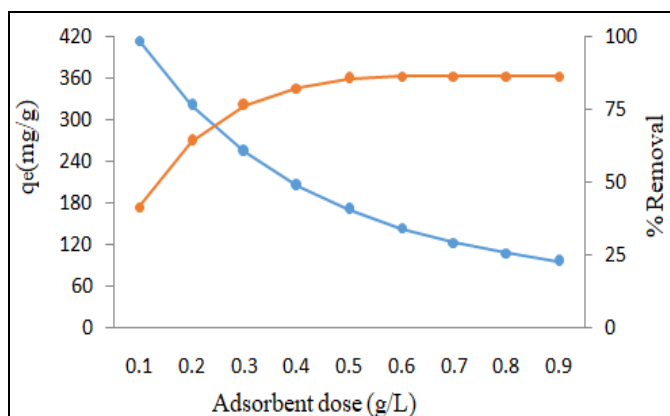


**FIG. 3: EFFECT OF ADSORBENT DOSE** ( $C_0 = 100$  mg/L,  $pH = 7$ , Contact time 75 min and Temp = 25 °C)

**Adsorption Kinetics:** Adsorption kinetics experiments were to study the impact of contact time and assess the dynamic characteristics. The amount of  $Fe_3O_4$ -GO was added to 200 mL CIP solution, adsorption amount at time  $t$  is calculated by the following formula:<sup>39</sup>

$$q_t = (C_0 - C_t)V / m$$

Where,  $q_t$  is the adsorption capacity of  $Fe_3O_4$ -GO at time  $t$  (mg/g),  $V$  is the volume of the solution (L),  $C_0$  is the initial concentration of CIP (mg/L)  $C_t$  is the concentration of the sample at time  $t$  (mg/L). Four kinetic equations: pseudo-first-order kinetic, pseudo-second-order kinetic, film diffusion model and intraparticle diffusion model were examined to fit the experimental data. They are listed below:

Pseudo-first order model:<sup>40</sup>

$$\ln(q_t - q_e) = \ln(q_e) - k_1 t$$

Pseudo-second order model:<sup>41</sup>

$$t/q_t = 1/(k_2 \cdot q_e) + t/q_e$$

Intra-particle diffusion model:<sup>42</sup>

$$q_t = K_3 t^{0.5} + C$$

Film diffusion model:<sup>43</sup>

$$\ln(1 - q_t/q_e) = -K_4 t + A$$

Where,  $q_t$  is the adsorption capacity of  $Fe_3O_4$ -GO at time  $t$  (mg/g),  $q_e$  is the equilibrium adsorption capacity of  $Fe_3O_4$ -GO (mg/g),  $K_1$  is the adsorption rate constant ( $h^{-1}$ ),  $K_2$  is the rate constant of second-order equation (g/mg. h),  $K_3$  is the intraparticle diffusion rate constant (mg/gmin<sup>1/2</sup>), and  $C$  is a constant that gives an idea about the thickness of the boundary layer (mg/g).  $K_4$  ( $h^{-1}$ ) and  $A$  are liquid film diffusion constants. Whether the dynamic model was suitable for describing the adsorption of CIP by  $Fe_3O_4$ -GO, normalized standard deviation  $\Delta q$ (%) was used for further authentication.  $\Delta q$  (%), given as:<sup>44,45</sup>

$$\Delta q = 100 \sqrt{\frac{\sum [(q_{exp} - q_{cal}) / q_{exp}]^2}{N - 1}}$$

Where  $N$  is the number of data,  $q_{exp}$  is the experimental adsorption capacity (mg/g)  $q_{cal}$  is the calculated adsorption capacity (mg/g).

The analysis results obtained by linear regression were summarized in **Table 2**. The Lower  $R^2$  and large  $\Delta q$  (%) showed that the pseudo-first-order kinetics model was not suitable for adsorption of CIP. The pseudo-second-order kinetic model can be fitted to the data, which the linear correlation coefficient is higher than 0.995 at all temperature **Fig. 4** and calculating the adsorption capacity and adsorption experiments relatively consistent.

Therefore the pseudo-second-order kinetic model was suitable to describe the adsorption process of CIP on  $Fe_3O_4$ -GO. The maximum adsorption quantity of CIP calculated by pseudo-second-order kinetic model and was 197 mg/g (273 K), 191.6 mg/g (288 K), 182.2 mg/g (303 K) and 172.6 mg/g (318 K). According to the secondary rate constant

( $K_2$ ) and initial adsorption rate (h), the adsorption rate slowed down with the temperature increasing. It indicated that the high temperature is not conducive to the adsorption. The adsorption process is usually controlled by either or both of them. In order to determine which one is the rate-controlling step, the intraparticle diffusion model and film diffusion model were used to fit to the

results of adsorption dates. If the linear plot of  $qt$  versus  $t^{1/2}$  is a straight line through the origin, indicating that the intraparticle diffusion is the only rate-controlling step. However, from the multi-linear curve obtained in the study, indicated that two or more steps occurred in the adsorption process<sup>44</sup>.

TABLE 2: KINETIC PARAMETERS FOR THE ADSORPTION OF CIP ONTO Fe<sub>3</sub>O<sub>4</sub>-GO

T (K)	q <sub>e</sub> exp (mg/g)	Pseudo-first order				Pseudo-second order			
		K <sub>1</sub>	q <sub>e</sub> (cal)	R <sup>2</sup>	Δq(%)	q <sub>e</sub> (cal)	R <sup>2</sup>	K <sub>2</sub>	Δq(%)
273	194.5	0.049	145.2	0.795	9.325	197	0.997	0.067	1.452
288	186.4	0.032	137.9	0.814	10.84	191.6	0.999	0.054	2.641
303	179.7	0.017	129.8	0.808	12.46	182.2	0.998	0.046	1.563
318	167.8	0.012	118.4	0.829	9.896	172.6	0.997	0.022	1.072
		Intra-particle diffusion model			Liquid film diffusion				
		K <sub>3</sub>	C	R <sup>2</sup>	Δq(%)	K <sub>4</sub>	A	R <sup>2</sup>	Δq(%)
273		14.12	69.45	0.941	4.45	0.244	0.096	0.924	3.45
288		16.44	62.75	0.952	3.89	0.228	0.117	0.913	2.24
303		17.25	58.94	0.938	5.11	0.212	0.145	0.889	2.88
318		19.16	53.12	0.942	3.27	0.195	0.168	0.927	1.93

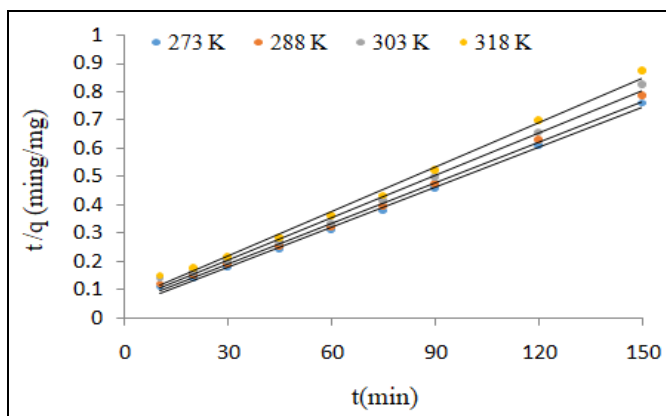


FIG. 4: PSEUDO-SECOND ORDER KINETICS MODELS FOR THE ADSORPTION OF CIP ADSORPTION

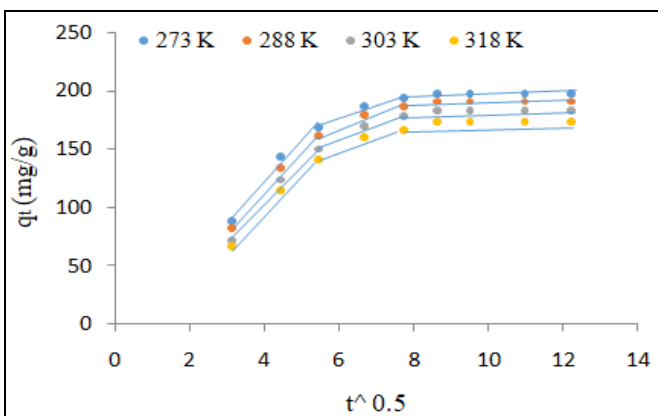


FIG. 5: INTRAPARTICLE DIFFUSION KINETICS MODELS FOR THE ADSORPTION OF CIP ADSORPTION

As seen in Fig. 5, the initial slope was big, which mean the adsorption rate was fast. That might be the surface adsorption or transient absorption. The second part was gradually adsorbed phase, which the liquid film diffusion was the main controlling step. The third step is the equilibrium period, as the concentration of adsorbate in solution was very low; the intra-particle diffusion was not the controlling step anymore.

The values of  $K_3$  and  $C$  in intra-particle diffusion were obtained by the second curve.  $C$  was used to describe the thickness of the boundary layer. The increasing value of  $C$  showed that the thickness of the boundary layer increased. As seen from the result, the thickness of the boundary layer increased

with the increasing temperature. In liquid film diffusion model, with the increasing of temperature, the value of  $K_4$  decreased. That indicated that the high temperature was adverse to liquid film diffusion. As temperatures went up, liquid film diffusion would become the limit factor.

**CONCLUSION:** Environmental pollution caused by industrial effluents is an important issue. Biosorption of CIP from aqueous solution using Fe<sub>3</sub>O<sub>4</sub>-GO was investigated in a batch mode. The results showed that increasing the dose of the adsorbent and the contact time increased the CIP removal. So with the increase in the absorbent dosage from 0.1 to 0.9 g/L, the percentage of removal increases from 41.4 to 86.8% at initial CIP

concentration 100 mg/L, whereas adsorption capacity decreases from 414 to 86.3 mg/g.

On the other hand, kinetic parameters have been investigated with pseudo-first-order, pseudo-second-order, intra-particle diffusion model and liquid film diffusion. The result of experimental data indicates that the pseudo second-order equation fit better than the other kinetics.

**ACKNOWLEDGEMENT:** The authors are grateful to the Zahedan University of Medical Sciences for the financial support of this study (Project No. 9325).

**CONFLICTS OF INTEREST:** Authors have declared that no competing interests exist.

## REFERENCES:

- Balarak D and Mostafapour FK: Batch equilibrium, kinetics and thermodynamics study of sulfamethoxazole antibiotics onto *Azolla filiculoides* as a novel biosorbent. *British J of Pharmaceutical Research* 2016; 13(2): 1-14.
- Farzadkia M, Esrafil A, Yang JK and Siboni MS: Photocatalytic degradation of metronidazole with illuminated TiO<sub>2</sub> nanoparticles. *Journal of Environmental Health Science and Engineering* 2015; 13: 35-44.
- Ahmadi S, Banach A and Mostafapour FK: Study survey of cupric oxide nanoparticles in removal efficiency of ciprofloxacin antibiotic from aqueous solution: Adsorption isotherm study. *Desalination and Water Treatment* 2017; 89: 297-03.
- Rahmani K, Faramarzi M, Mahvi AH, Gholami M, Esrafil A, Forootanfar H and Farzadkia M: Elimination and detoxification of sulfathiazole and sulfamethoxazole assisted by laccase immobilized on porous silica beads. *International Biodeterioration and Biodegradation* 2015; 97: 107-14.
- Hu D and Wang L: Adsorption of amoxicillin onto quaternized cellulose from flax noil: Kinetic, equilibrium and thermodynamic study. *J Taiwan Inst Chem Eng* 2016; 64: 227-34.
- Yu F, Li Y, Han S and Ma J: Adsorptive removal of antibiotics from aqueous solution using carbon materials. *Chemosphere* 2016; 153: 365-85.
- Balarak D, Mostafapour FK and Joghataei A: Experimental and kinetic studies on penicillin G Adsorption by *Lemna minor*. *British Journal of Pharmaceutical Research* 2016; 9(5): 1-10.
- Chayid MA and Ahmed MJ: Amoxicillin adsorption on microwave prepared activated carbon from *Arundo donax* Linn: isotherms, kinetics, and thermodynamics studies. *J Environ Chem Eng* 2015; 3: 592-01.
- Mahvi AH, Mostafapour FK and Balarak D: Biosorption of tetracycline from aqueous solution by *A. filiculoides*: equilibrium kinetic and thermodynamics studies. *Fresenius Environmental Bulletin* 2018; 27(8): 5759-67.
- Garoma T, Umamaheshwar SH and Mumper A: Removal of sulfadiazine, sulfamethizole, sulfamethoxazole, and sulfathiazole from aqueous solution by ozonation. *Chemosphere* 2010; 79: 814-20.
- Balarak D, Mostafapour FK, Bazrafshan E and Saleh, Tawfik A: Studies on the adsorption of amoxicillin on multi-wall carbon nanotubes. *Water Science & Technology* 2017; 16: 1599-06.
- Balarak D and Azarpira H: Rice husk as a biosorbent for antibiotic metronidazole removal: Isotherm studies and model validation. *International Journal of Chem Tech Research* 2016; 9(7): 566-73.
- Zhu XD, Wang YJ, Sun RJ and Zhou DM: Photocatalytic degradation of tetracycline in aqueous solution by nanosized TiO<sub>2</sub>. *Chemosphere* 2013; 92: 925-32.
- Pouretedal HR and Sadegh N: Effective removal of amoxicillin, cephalixin, tetracycline and penicillin G from aqueous solutions using activated carbon nanoparticles prepared from vine wood. *J Water Process Eng* 2014; 1: 64-73.
- Balarak D, Azarpira H and Mostafapour FK: Study of the adsorption mechanisms of cephalixin on to *Azolla filiculoides*. *Der Pharma Chemica* 2016; 8(10): 114-21.
- Balarak D, Mostafapour FK and Azarpira H: Adsorption kinetics and equilibrium of ciprofloxacin from aqueous solutions using hazelnut activated carbon. *British Journal of Pharmaceutical Research* 2016; 13(3): 1-14.
- Zhang CL, Qiao GL, Zhao F and Wang Y: Thermodynamic and kinetic parameters of ciprofloxacin adsorption onto modified coal fly ash from aqueous solution. *J of Molecular Liquids* 2011; 163(1): 53-56.
- Pezoti O, Cazetta AL, Bedin KC, Souza LS and Martins AC: NaOH-activated carbon of high surface area produced from guava seeds as a high-efficiency adsorbent for amoxicillin removal: Kinetic, isotherm and thermodynamic studies. *Chem Eng J* 2016; 288: 778-788
- Balarak D, Azarpira H and Mostafapour FK: Adsorption isotherm studies of tetracycline antibiotics from aqueous solutions by maize stalks as a cheap biosorbent. *International Journal of Pharmacy & Technology*.2016; 8(3): 16664-75.
- Seo PW, Khan NA and Jhung SH: Removal of nitroimidazole antibiotics from water by adsorption over metal-organic frameworks modified with urea or melamine. *Chemical Engineering J* 2017; 315: 92-00.
- Sepehr MN, Al-Musawi TJ, Ghahramani E, Kazemian H and Zarrabi M: Adsorption performance of magnesium/aluminum layered double hydroxide nanoparticles for metronidazole from aqueous solution. *Arabian Journal of Chemistry* 2017; 10: 611-23.
- Zhang L, Song X, Liu X, Yang L, Pan F and Lv J: Studies on the removal of tetracycline by multi-walled carbon nanotubes. *Chem Eng J* 2011; 178: 26-33.
- Azarpira H, Mahdavi Y and Khaleghi O: Thermodynamic studies on the removal of metronidazole antibiotic by multi-walled carbon nanotubes. *Der Pharmacia Lettre* 2016; 8(11): 107-13.
- Peterson JW, Petrasky LJ, Seymour MD, Burkhardt RS and Schuilinga AB: Adsorption and breakdown of penicillin antibiotic in the presence of titanium oxide nanoparticles in water. *Chemosphere* 2012; 87(8): 911-7.
- Chen WR and Huang CH: Adsorption and transformation of tetracycline antibiotics with aluminium oxide. *Chemosphere* 2010; 79: 779-85.
- Xu L, Pan J, Dai J, Li X, Hang H, Cao Z and Yan Y: Preparation of thermal-responsive magnetic molecularly imprinted polymers for selective removal of antibiotics from aqueous solution. *Journal of Hazardous Materials* 2012; 233-234: 48-56.
- Balarak D and Mostafapour FK: Photocatalytic degradation of amoxicillin using UV/synthesized NiO

- from pharmaceutical wastewater. Indonesian Journal of Chemistry 2019; 19(1): 211-18.
28. Yao Y, Miao S, Liu S, Ma LP, Sun H and Wang S: Synthesis, characterization, and adsorption properties of magnetic Fe<sub>3</sub>O<sub>4</sub>-graphene nanocomposite. Chemical Engineering Journal 2012; 184: 326-32.
  29. Sohail M, Saleem M, Ullah S, Saeed N, Afridi A and Khan M: Synthesis of graphene oxide using modified hummers method solvent influence. Procedia Engineering 2017; 184: 469-77.
  30. Zazouli MA, Mahvi AH, Dobaradaran S, Barafrashtepour M, Mahdavi Y and Balarak D: Adsorption of fluoride from aqueous solution by modified *Azolla filiculoides*. Fluoride 2014; 47(4): 349-58.
  31. Carvalho IT and Santos L: Antibiotics in the aquatic environments: a review of the European scenario. Environ Int 2016; 94: 736-57.
  32. Diyanati RA, Yousefi Z and Cherati JY: The ability of *Azolla* and *Lemna minor* biomass for adsorption of phenol from aqueous solutions. J Mazand Uni Med Sci 2013; 23: 17-23.
  33. Liu H, Hu Z, Liu H, Xie H, Lu S, Wang Q and Zhang J: Adsorption of amoxicillin by Mn-impregnated activated carbons: Performance and mechanisms. RSC Adv 2016; 6: 11454-60.
  34. Peng X, Hu F, Dai H and Xiong Q: Study of the adsorption mechanism of ciprofloxacin antibiotics onto graphitic ordered mesoporous carbons. J Taiwan Inst Chem Eng 2016; 8: 1-10.
  35. Balarak D and Azarpira H: Photocatalytic degradation of sulfamethoxazole in water: an investigation of the effect of operational parameters. International Journal of Chem Tech Research 2016; 9(12): 731-8.
  36. Balarak D, Bazrafshan E, Mahdavi Y and Lee SM: Kinetic, isotherms and thermodynamic studies in the removal of 2-chlorophenol from aqueous solution using modified rice straw. Desalination and water treatment 2017; 63: 203-11.
  37. Kam SK and Lee MG: Response surface modeling for the adsorption of dye Eosin Y by activated carbon prepared from waste citrus peel. Appl Chem Eng 2018; 29(3): 270-77.
  38. Balarak D, Mostafapour FK, Lee SM and Jeon C: Adsorption of bisphenol a using dried rice husk: equilibrium, kinetic and thermodynamic studies. Appl Chem Eng 2019; 30(3): 316-23.
  39. Gao Y, Li Y, Zhang L, Huang H, Hu J, Shah SM and Su X: Adsorption and removal of tetracycline antibiotics from aqueous solution by graphene oxide. J Colloid Interface Sci 2012; 368: 540-46.
  40. Rostamian R and Behnejad H: A comparative adsorption study of sulfamethoxazole onto graphene and graphene oxide nanosheets through equilibrium, kinetic and thermodynamic modeling. Process Safety and Environmental Protection 2016; 102: 20-29.
  41. Bazrafshan E, Panahi AH, Kamani H and Mahvi AH: Fluoride removal from aqueous solutions by cupric oxide nanoparticles. Fluoride 2016; 49(3): 233-44.
  42. Yao Y, He B, Xu F and Chen X: Equilibrium and kinetic studies of methyl orange adsorption on multi-walled carbon nanotubes. Chemical Engineering Journal 2011; 170: 82-89.
  43. Balarak D, Mahdavi Y, Bazrafshan E and Mahvi AH: Kinetic, isotherms and thermodynamic modeling for adsorption of acid blue 92 from aqueous solution by modified *Azolla filiculoides*. Fresenius Environmental Bulletin 2016; 25(5): 1321-30.
  44. Bazrafshan E, Mahvi AH, Havangi M and Panahi AH: Adsorptive removal of nitrate from aqueous environments by cupric oxide nanoparticles: kinetics, thermodynamics and isotherm studies. Fresenius Environmental Bulletin 2018; 27(8): 5669-5678.
  45. Zazouli MA, Mahvi AH and Mahdavi Y: Isothermic and kinetic modeling of fluoride removal from water by means of the natural biosorbents sorghum and canola. Fluoride. 2015; 48(1): 15-22.

**How to cite this article:**

Balarak D, Zafariyan M and Chandrika K: Adsorption of ciprofoxacin from aqueous solution onto Fe<sub>3</sub>O<sub>4</sub>/graphene oxide nanocomposite. Int J Pharm Sci & Res 2020; 11(1): 268-74. doi: 10.13040/IJPSR.0975-8232.11(1).268-74.

All © 2013 are reserved by International Journal of Pharmaceutical Sciences and Research. This Journal licensed under a Creative Commons Attribution-NonCommercial-ShareAlike 3.0 Unported License.

This article can be downloaded to **Android OS** based mobile. Scan QR Code using Code/Bar Scanner from your mobile. (Scanners are available on Google Play store)